Ah Receptor Nuclear Translocator Protein Heterogeneity Is Altered after Heterodimerization with the *Ah* Receptor†

Jo Chao Tsai and Gary H. Perdew*

Department of Veterinary Science, The Pennsylvania State University, University Park, Pennsylvania 16802

Received April 16, 1997⊗

ABSTRACT: The *Ah* receptor (AhR) and the *Ah* receptor nuclear translocator (ARNT) are capable of forming a transcriptionally active heterodimeric complex. The biochemical events that are required for dimerization and transactivation are not fully understood. The purpose of this study was to determine whether covalent modifications of ARNT occur between ARNT existing in the monomeric form and after heterodimerization with the AhR and subsequent binding to DNA. Mouse hepatoma cell line 1c1c7 (Hepa 1) cytosol and ARNT immunoprecipitations were subjected to two-dimensional gel electrophoresis. ARNT was visualized with two antibodies, with distinct epitope specificity, and each detected a considerable level of charge heterogeneity. The p*I* range observed was 5.7−6.4, with the predominant form at a p*I* of 6.2. The AhR/ARNT heterodimer was immunoprecipitated from high-salt nuclear extract obtained from Hepa 1 cells treated with β-naphthoflavone using an anti-AhR polyclonal antibody. This immunoprecipitate was subjected to two-dimensional gel electrophoresis, and coimmunoprecipitated ARNT was visualized. The results indicated that ARNT complexed with the AhR in the nucleus has an isoform pattern shifted toward the basic end, with the predominant isoform having a p*I* of 6.8. Thus, a significant shift in p*I* occurs during the dimerization and/or after binding to DNA. *In vitro* transformation of the AhR with 2,3,7,8-tetrachlorodibenzo-*p*-dioxin in cytosol leads to heterodimerization with ARNT. Two-dimensional gel electrophoresis of ARNT coimmunoprecipitated with the AhR revealed the same isoform pattern as seen in cytosol. This would indicate that each isoform of ARNT is capable of heterodimerizing with the AhR *in vitro*. ARNT is a phosphoprotein, and the more acidic isoforms appear to have a higher level of phosphorylation.

Signal transduction by environmental pollutants, such as dioxins, related halogenated hydrocarbons, and polycyclic aromatic hydrocarbons is mediated by the AhR,[1] which elicits a plethora of biochemical and toxic responses [reviewed in Swanson and Bradfield (1993)]. The latent form of AhR is located in the cytoplasm of untreated cells in complex with the molecular chaperone hsp90 and p43 (Perdew, 1988; Chen & Perdew, 1994). Upon binding a ligand, such as TCDD, the AhR translocates to the nucleus, hsp90 dissociates, and the AhR heterodimerizes with ARNT, a constitutively nuclear protein (Pollenz *et al.*, 1994; Hord & Perdew, 1994). The AhR/ARNT heterodimer recognizes the cis-acting DNA enhancer sequences known as XREs, localized upstream of certain genes, such as CYP1A1, and activates their transcription (Reyes *et al.*, 1992; Fujii-Kuriyama *et al.*, 1992; Hapgood *et al.*, 1989; Matsushita *et al.*, 1993). The specific series of biochemical events that lead to formation of AhR/ARNT and subsequent formation of a transcriptionally active complex are poorly understood. In particular, the role of ARNT in regulating heterodimer formation has not been elucidated.

Both *Ah* receptor and ARNT belong to a family of ligand-activated transcription factors consisting of a basic helix−loop−helix (bHLH) structural motif contiguous with a PAS domain (Burbach *et al.*, 1992). Various members of this family include Per, Sim, ARNT, AhR, and the newly discovered HIF-1 (Wang *et al.*, 1995). The basic regions of AhR and ARNT are responsible for XRE binding (Reisz-Porszasz *et al.*, 1994), and the HLH region and PAS domain contribute to heterodimerization between the two proteins (Lindebro *et al.*, 1995; Fukunaga *et al.*, 1995; Huang *et al.*, 1993). The transactivation domain for both AhR and ARNT resides in the C-terminal half of the protein (Jain *et al.*, 1994; Sogawa *et al.*, 1995a). ARNT is now emerging as a central dimerization partner of the PAS family of transcriptionally active proteins. In addition to the AhR, ARNT can heterodimerize with HIF-1 (Wang *et al.*, 1995; Li *et al.*, 1996) and Sim-1, as well as form potential homodimers to bind to an E-box motif (Sogawa *et al.*, 1995b; Antonsson *et al.*, 1995). Therefore, it is important to understand potential mechanism(s) of ARNT regulation including dimerization and transactivation. Very little is known about the biochemistry of ARNT other than it is localized in the nucleus of

† This work was supported in part by National Institute of Environmental Health Science Grant ES-04869.

* Corresponding author. Fax: 814-863-6140. Electronic mail address: ghp2@psu.edu.

⊗ Abstract published in *Advance ACS Abstracts,* July 1, 1997.

[1] Abbreviations: AhR, *Ah* receptor (aryl hydrocarbon receptor); ARNT, *Ah* receptor nuclear translocator protein; hsp90, 90-kDa heat shock protein; CYP1A1, structural gene for cytochrome P-4501A1; TCDD, 2,3,7,8-tetrachlorodibenzo-*p*-dioxin; XRE, xenobiotic responsive element; bHLH, basic helix−loop−helix; Per, period; Sim, single-minded; PAS, Per-AhR-ARNT-Sim; HIF-1, hypoxia-inducible factor 1; GAM, goat anti-mouse; Hepa 1, mouse hepatoma cell line 1c1c7; α-MEM, α-minimum essential medium; FBS, fetal bovine serum; βNF, β-naphthoflavone; DMSO, dimethyl sulfoxide; IEF, isoelectric focusing; SDS, sodium dodecyl sulfate; PAGE, polyacrylamide gel electrophoresis; NP-40, nonidet P-40; PVDF, poly(vinylidene difluoride); DTT, dithiothreitol; mAb, monoclonal antibody; pAb, polyclonal antibody; PBS, phosphate-buffered saline.

S0006-2960(97)00891-X CCC: $14.00

cultured cells and that it exists predominantly in a monomeric form (Hord & Perdew, 1994).

Two-dimensional gel electrophoresis is a powerful technique to separate proteins with high resolution and sensitivity. It can resolve proteins differing in a single charge and consequently can be used in the analysis of posttranslational modifications which often result in an alteration in net charge (O'Farrell, 1975). Conserved charge heterogeneity in the AhR was observed among species, which suggests a possible role in its function (Perdew, 1991; Perdew & Hollenback, 1990). The purpose of this study was to determine whether phosphorylation or other covalent modifications, which would result in a change in net charge, occur between ARNT in the monomeric form and ARNT after heterodimerization with the AhR and subsequent binding to DNA. We report here for the first time that ARNT has considerable charge heterogeneity with multiple isoforms being detected in Hepa 1 cells. A significant shift in the p*I* of ARNT was also observed after heterodimerization with the liganded AhR in the nucleus. In addition, we directly demonstrate that ARNT is a phosphoprotein and that the charge heterogeneity observed appears to be, at least in part, due to phosphorylation. The data presented here should complement phosphorylation studies examining the role of phosphorylation in regulating the activity of ARNT.

EXPERIMENTAL PROCEDURES

Materials. Biotin-SP-conjugated goat anti-mouse (GAM) IgG, peroxidase-conjugated streptavidin, and peroxidase-conjugated donkey anti-rabbit IgG were purchased from Jackson Immunoresearch Laboratories, Inc. (West Grove, PA). Acrylamide and dithiothreitol were obtained from Research Organics (Cleveland, OH). Bio-Lyte 3/10 ampholytes were obtained from Bio-Rad Laboratories (Hercules, CA). BCA protein assay reagents were obtained from Pierce (Rockford, IL). Rabbit polyclonal anti-ARNT and anti-AhR antibodies were generous gifts from Richard Pollenz (Pollenz *et al.*, 1994). The ARNT expression vector pSV-Sport1-ARNT was obtained from Christopher Bradfield (Dolwick *et al*., 1993). pcDNA1/mARNT plasmid construct was obtained from Dr. Oliver Hankinson (Reisz-Porszasz *et al*., 1994). The Hepa 1 cell line was obtained from Dr. James Whitlock (Stanford University). COS-1 cells were purchased from ATCC (Rockville, MD). Fetal bovine serum was purchased from Hyclone Lab (Logan, UT). Vent DNA polymerase, restriction endonucleases, and other DNA-modifying enzymes were from New England Biolabs (Beverly, MA). [^{32}P]Phosphorus orthophosphate (370 MBq/mL, 10 mCi/mL) was purchased from Amersham (Arlington Heights, IL). Oligonucleotides for PCR amplification were synthesized by GENOSYS (Woodlands, TX). Flag peptide and anti-flag M2 monoclonal antibody affinity gel were obtained from Kodak Imaging Systems (Rochester, NY). Lipofectamine reagent and opti-MEM were obtained from Life Technologies (Gaithersburg, MD). All other chemicals were from Sigma unless otherwise noted.

Cell Culture and Preparation of Cellular Extracts. Hepa 1 cell line was grown in α-minimum essential medium (α-MEM) supplemented with 8% FBS, 100 international units/mL penicillin, and 0.1 mg/mL streptomycin at 37 °C in 94% air, 6% CO_2. Hepa 1 cells were grown to 70−80% confluency and harvested essentially as described (Chen & Perdew, 1994). The cells were resuspended in MENG (25 mM MOPS, 2 mM EDTA, 0.02% NaN_3, and 10% glycerol, pH 7.5) or MENG plus 10 mM sodium pyrophosphate, 20 mM sodium molybdate, 10 mM NaF, and 0.4 mM sodium vanadate (MENGPI) and homogenized in a Dounce homogenizer. The same set of phosphatase inhibitors were used throughout the experiments. The cell homogenate was centrifuged at 3000*g* for 10 min, and the supernatant was removed and centrifuged at 100000*g* for 60 min to yield the cytosolic fraction. The 3000*g* pellet was washed 3 times with MENG or MENGPI before being extracted with 500 mM NaCl in MENG or MENGPI for 1 h on ice. After centrifugation at 100000*g* for 30 min, the supernatant was taken as the high-salt nuclear extract.

For βNF treatment experiments, Hepa 1 cells were grown to 70−80% confluency, and were treated with 10 μM βNF for 1 h. For the control experiments, equal amounts of DMSO were added to the media. The nuclear extract and cytosolic fraction were prepared as described above. Protein values for both the cytosolic fraction and the high-salt nuclear extract were determined by the BCA protein assay (Pierce).

Immunoprecipitations. ARNT was immunoprecipitated with a mouse mAb 2B10 against ARNT (Hord & Perdew, 1994). To 50 μL of GAM IgG (whole molecule)−agarose was added 5 μg of mAb 2B10 or a control mouse IgG, and the mixtures were incubated for 1 h on ice followed by two washes with MENG buffer. Hepa 1 cytosolic protein (400 μg) was added to each agarose pellet, and the mixtures were gently agitated on ice for 1−2 h. The sample was washed once with MENG buffer and twice with MENG + 500 mM NaCl and then washed with MENG before being solubilized in 50 μL of 2× lysis buffer [6% NP-40, 4% ampholyte Bio-Lyte (3/10), 0.14 M dithiothreitol, and 9.5 M urea]. The samples were saturated with urea before being loaded on the isoelectric focusing (IEF) gel.

In some cases, the cytosol was incubated with the gel in the presence of phosphatase inhibitors (MENGPI buffer), and the subsequent washes were performed with MENGPI and MENGPI + 500 mM NaCl. Immunoprecipitation of ARNT from the nuclear extract for both the control and the βNF-treated Hepa 1 cells was completed in a similar fashion, except 500 mM NaCl was included in the buffer. Each immunoprecipitation utilized 500 μg or 600 μg of nuclear extract proteins.

Ah receptor was coimmunoprecipitated from the nuclear extract of βNF-treated Hepa 1 cells with an anti-AhR polyclonal antibody, using the procedure similar to that described above. MENG or MENGPI with 500 mM NaCl were used in the incubation and washes.

Two-Dimensional Gel Electrophoresis. IEF−SDS−PAGE was performed essentially as described (Perdew & Hollenback, 1990), with a few modifications. IEF gels were formed with the following final composition: 2.0% pH 3.0−10 ampholytes, 2% NP-40 (w/v), 9 M urea, 3.4% acrylamide, 0.1% bis(acrylamide). Samples were applied to the acidic end, and the gels were run at 200 V for 2 h, followed by 300 V for 14 h, and finally 800 V for 2 h. Focused gels were pushed out of the glass tubes from the basic end with a syringe filled with distilled water. Either the whole gel or the gel that was cut 6 cm from the acidic end was transferred into 10 mL of equilibration buffer (2.8% SDS, 0.1% bromophenol blue, and 70 mM Tris-HCl, pH 6.8) and gently agitated for 5 min. The IEF gels were sealed with 1% hot

agarose in equilibration buffer on top of a 1.5 mm thick, 7.5% polyacrylamide gel with a 2 cm 3% stacking gel and current applied at 10 mA/gel for 2 h, followed by 20 mA/gel, essentially as described (Perdew & Hollenback, 1990).

The pH gradient was determined by slicing the IEF gel into 0.5 cm segments, starting from the acidic end, and placing them in 1.5 mL microfuge tubes with 0.4 mL of deionized water. The set of tubes was allowed to sit for 12−24 h before the pH values were measured. Each pH value was an average of four measurements from independent experiments. Individual p*I* values of ARNT were determined using these pH gradients versus distance from the acidic end measured on the two-dimensional gel.

In Vitro Expression of ARNT. *In vitro* transcription and translation of pSV-Sport-ARNT were carried out using the TNT SP6-coupled rabbit reticulocyte lysate and wheat germ extract systems (Promega). The reaction was carried out as recommended using 20 μCi of [^{35}S]methionine/50 uL reaction mixture (Promega). IEF−SDS−PAGE of *in vitro* translated ARNT was performed using 10 μL of rabbit reticulocyte lysate and 25 μL of the wheat germ extract translated ARNT, mixed with an equal volume of 2× lysis buffer as described above. Autoradiography was performed to visualize radiolabeled ARNT after the proteins were electrotransferred to a PVDF membrane.

In Vitro Transformation of AhR with TCDD. AhR can be induced to form a heterodimer with ARNT when treated with TCDD *in vitro*. Hepa 1 cytosol (600 μg) was diluted in MENG to 2 mg/mL in the presence of 1 mM dithiothreitol. *In vitro* transformation was performed in Hepa 1 cytosol when 20 nM TCDD (disolved in DMSO) was added. An equal amount of DMSO was added in the control experiments, with a maximum DMSO concentration of 0.16%. The reaction mixtures were incubated at 30 °C for 2 h. AhR/ARNT heterodimer was then immunoprecipitated with an anti-AhR rabbit polyclonal antibody, or with a control rabbit IgG absorbed to the anti-rabbit IgG−agarose as described. The final pellet was washed with MENG plus 500 mM NaCl twice, followed by two washes with MENG buffer, before being subjected to SDS−PAGE or IEF−SDS−PAGE. ARNT was also immunoprecipitated from TCDD- or DMSO-treated Hepa 1 cytosol (400 μg) using mAb 2B10 absorbed to anti-mouse IgG−agarose. Each immunoprecipitate was subjected to IEF−SDS−PAGE.

Plasmid Construction. ARNT/flag cDNA was amplified by polymerase chain reaction (PCR) using pcDNA1/mARNT as a template. Two oligonucleotides, a T7 promoter forward primer (5′-TAATACGACTCACTATAGGG-3′) and an ARNT/flag reverse primer (5′-CCGCTCGAGTCACTTGTCATCGTCGTCCTTGTAGTCTTCTGAAAAGGGGGGAAA-3′), were used to amplify and add a flag sequence to the 3′ terminus of the mARNT gene using standard PCR techniques. The resulting PCR product was digested with *Hin*dIII and *Xho*I and subcloned in the *Hin*dIII/*Xho*I sites of pcDNA3 vector (Invitrogen). The nucleotide sequence was confirmed by nucleotide sequencing.

Transient Transfection and [^{32}P]Orthophosphate Labeling of Transfected Cells. COS-1 cells were cultured in αMEM + 10% FBS. COS-1 cells that are 50−60% confluent were transiently transfected with mARNT/flag/pcDNA3 using lipofectamine reagent diluted in opti-MEM essentially as described by the manufacturer. For each transfection, 12 μg of DNA/40 μL lipofectamine complex was added to the cells in a 75 cm^2 flask with serum-free opti-MEM. Eleven hours after incubating with DNA−lipofectamine complexes, an equal volume of opti-MEM containing 20% FBS was added to the cells, and incubated for another 4 h. The transfected COS-1 cells were rinsed and preincubated for 1 h at 37 °C in phosphate-free Eagle's minimum essential medium containing 8% dialyzed FBS. The cells were then replaced with the fresh media, and 150 μCi/mL [^{32}P]-orthophosphate was added. The cells were labeled for 20 h followed by trypsinization of the cells. After washing with PBS, the cells were lysed with 1% NP-40 in MENGPI containing 1.25 μg/mL leupeptin, 1.8 μg/mL pepstatin A, and 25 μg/mL aprotonin. The cell lysate was subjected to ultracentrifugation, and the supernatant was collected.

Immunoprecipitation of Radiolabeled ARNT and Gel Electrophoresis. The cell lysate from mARNT/flag/pcDNA3-transfected COS-1 cells was subjected to immunoprecipitation with anti-flag M2 mAb. The cell lysate (300 μg) was added to 25 μl of anti-flag M2 affinity gel. The final buffer composition during immunoprecipitation contained MENGPI + protease inhibitor mixture, 1% NP-40, and 250 mM NaCl, pH 7.3. For control experiments, the anti-flag M2 affinity gel was first preincubated for 1 h with 90 nmol of the flag peptide (DYKDDDDK) before the cell lysate was added. The immunoprecipitation reactions were run overnight on ice. The immunoprecipitations were washed twice with MENGPI plus 500 mM NaCl. The gels were transferred onto a sucrose cushion (1 mL of 1 M sucrose + 1% NP-40 + 500 mM NaCl in MENG), and pelleted at 4000 rpm for 10 min. The gel was then washed twice with 0.5% SDS, 2% NP-40, and 500 mM NaCl in MENG, each incubated for 10 min, and finally twice with MENG prior to being subjected to the SDS−PAGE, or IEF−SDS−PAGE, gels. The proteins were transferred to a PVDF membrane, and the radiolabeled proteins were visualized by autoradiography. Expressed ARNT/flag was visualized on protein blots with mAb 2B10 and GAM−peroxidase conjugate.

Immunodetection. Proteins were transferred from polyacrylamide gels to PVDF membranes at 8 V for 6 h in a Genie Blotting unit (Idea Scientific, Minneapolis, MN). After the nonspecific binding sites were blocked with 3% bovine serum albumin, 0.05% Tween 20, in phosphate-buffered saline, pH 7.4, at room temperature for 1 h, the blot was incubated with primary anti-ARNT mouse mAb 2B10 (1/1000 dilution) or rabbit polyclonal antibody (0.4 μg/mL). The mAb 2B10/ARNT complexes were detected by incubation with secondary biotin-SP-conjugated GAM IgG, followed by streptavidin-conjugated peroxidase complex. When primary anti-ARNT rabbit polyclonal antibody was used, donkey anti-rabbit IgG-conjugated peroxidase complex was used for detection. Peroxidase was visualized with Vector VIP kit (Vector Laboartories, Burlingame, CA). Blots were washed 5 times with 0.1% bovine serum albumin, 0.05% Tween 20, in phosphate-buffered saline, pH 7.4, for 5 min between each incubation step.

RESULTS AND DISCUSSION

ARNT shows considerable charge heterogeneity in Hepa 1 cells. Upon homogenization, almost all of the ARNT present in the cell is found in the cytosolic fraction apparently leaches out of nuclei (Hord & Perdew, 1994). Cytosolic extracts from Hepa 1c1c7 cells were subjected to IEF−SDS−

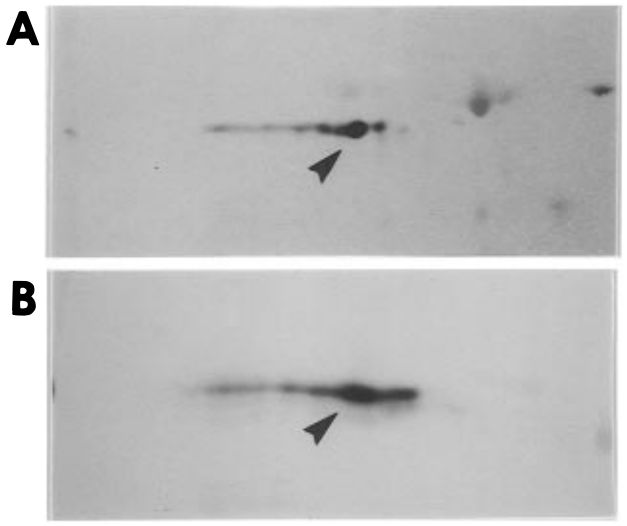

FIGURE 1: Heterogeneity of ARNT in Hepa 1 cytosol determined by IEF−SDS−PAGE. Hepa 1 cytosol was subjected to IEF−SDS−PAGE and visualized with anti-ARNT mAb 2B10 (panel A) and rabbit polyclonal antibody (panel B). The predominant isoform of ARNT is marked by the arrowhead. For all IEF−SDS−PAGE, the first-dimension IEF gels were run from left to right with the acidic end of the pH gradient on the left and the basic end on the right. Second-dimension SDS gels were run from top to bottom. Results shown are from a representative experiment repeated at least 4 times.

PAGE, followed by electrotransfer to membrane. ARNT was visualized with both mAb 2B10 and anti-ARNT affinity-purified rabbit polyclonal antibodies. Each antibody revealed considerable charge heterogeneity (Figure 1). The rationale for using two distinct anti-ARNT antibodies was to test for any artifacts that may be associated with the blot visualization and immunoprecipitation assay systems. Each antibody preparation was raised against different epitopes. MAb 2B10 was raised against a carboxyl-terminal 19 amino acid peptide hapten (Hord & Perdew, 1994). The rabbit polyclonal antibody was against a His-tagged protein corresponding to amino acids 318−773 of human ARNT (Pollenz et al., 1994). It was anticipated that the rabbit polyclonal antibody would recognize multiple epitopes and thus be more sensitive than mAb 2B10. The charge heterogeneity seen after IEF−SDS−PAGE is comparable between blots visualized with these two antibodies. However, the blot visualized with rabbit polyclonal antibody did show more isoforms, probably due to its greater sensitivity (Figure 1B). The p*I* values for those isoforms were determined using a pH profile of the IEF gel generated as described under Experimental Procedures. The pH gradient of pH 5.0−8.5 was obtained and was linear versus distance.[2] The pH profile was derived from at least four separate experiments. The predominant ARNT isoform has a p*I* of 6.2 (marked by an arrowhead), while there is a trail of isoforms more toward the acidic end with p*I* values ranging from 5.4 to 6.4. Including phosphatase inhibitors when preparing cellular extracts and in immunoprecipitations did not show any apparent differences in the data presented throughout this report. Other spots on the blot visualized with 2B10 (Figure 1A) were attributed to background when compared with a control mouse IgG as the primary antibody on a duplicate blot.[2]

Another approach to carefully examine the level of ARNT charge heterogeneity is to examine immunoprecipitations on protein blots. ARNT was immunoprecipitated from Hepa 1 cytosol with mAb 2B10, and visualized on a protein blot with either mAb 2B10 or rabbit polyclonal antibody. Considerable charge heterogeneity was observed with both antibodies (Figure 2). In addition, there were comparably more isoforms visualized toward the basic end of the IEF gel, although the p*I* of the predominant form remained the same compared to the total cytosol sample visualized in Figure 1. The reason for the detection of more isoforms toward the basic end of the immunoprecipitated samples might be due to mAb 2B10 preference for certain isoforms. ARNT immunoprecipitated with rabbit polyclonal anti-ARNT antibody revealed a similar pattern of charge heterogeneity compared to the cytosol samples (data not shown). The p*I* for ARNT isoforms visualized with mAb 2B10 ranged from 6.0 to 6.8, with the p*I* of the predominant isoform at 6.2 (Figure 2A). The blot visualized with the rabbit polyclonal antibody showed the same p*I* for the predominant isoform, while there is a trailing of p*I* values ranging from 5.4 to 6.8 (Figure 2B). The rabbit polyclonal antibody is more sensitive than mAb 2B10. More isoforms were detected in immunoprecipitations with the rabbit polyclonal antibody, and the isoforms tended to spread out on the IEF gel. The results with both visualization systems which recognize distinct epitopes of ARNT clearly indicate that ARNT has significant charge heterogeneity with at least one predominant isoform in Hepa 1 cells. This charge heterogeneity is apparently indicative of different levels of post-translational modification, with the most likely modification being phosphorylation. The calculated p*I* of ARNT is 6.8, while the experimentally determined p*I* of the major isoform is 6.2; this is consistent with posttranslational modifications occurring after translation resulting in a shift toward the more acidic isoforms.

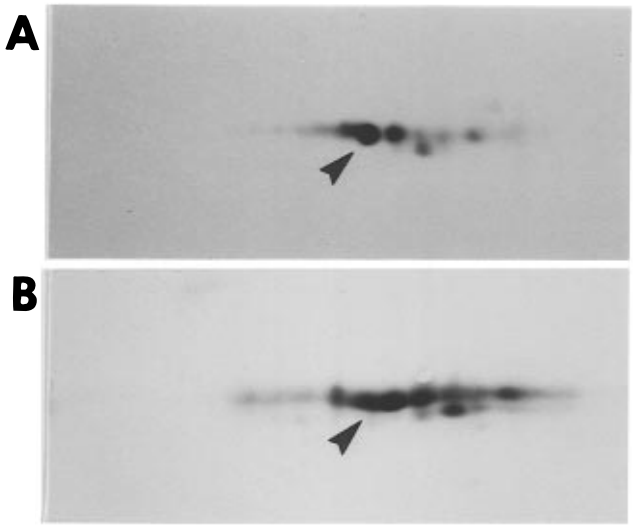

FIGURE 2: IEF−SDS−PAGE analysis of ARNT immunoprecipitates of Hepa 1 cytosol. ARNT was immunoprecipitated from 400 μg of Hepa 1 cytosol with mAb 2B10, subjected to IEF−SDS−PAGE, and visualized after protein blotting using mAb 2B10 (panel A) or a rabbit polyclonal Ab (panel B) as the primary Ab. The predominant isoform of ARNT was indicated with an arrowhead, the same isoform marked in Figure 1.

ARNT That Tightly Associates with the AhR in the Nucleus after βNF Treatment Undergoes a Significant Shift in pI. After treatment with 10 μM βNF for 1 h, ARNT was coimmunoprecipitated with an anti-AhR polyclonal antibody

[2] Unpublished observations.

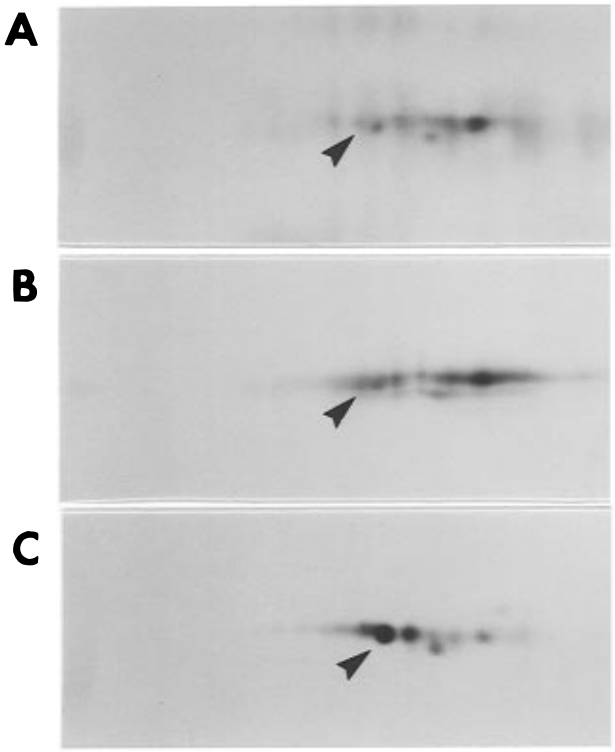

FIGURE 3: IEF−SDS−PAGE analysis of ARNT that was coimmunoprecipitated with AhR from nuclear extract of Hepa 1 cells after βNF treatment. Hepa 1 cells were treated with 10 μM μNF for 1 h, nuclear extract was prepared as described, and the AhR/ARNT heterodimer was immunoprecipitated with a mouse anti-AhR polyclonal Ab. ARNT was visualized with mAb 2B10 (panel A) or rabbit polyclonal (panel B) Abs on a protein blot. Cytosolic ARNT was immunoprecipitated with mAb 2B10 and was subjected to IEF−SDS−PAGE and visualized with mAb 2B10 (panel C). The position of the predominant ARNT isoform marked in Figure1 and Figure 2 was labeled with an arrowhead.

from nuclear extracts of Hepa 1 cells. This will coimmunoprecipitate ARNT that has heterodimerized with the AhR in the nucleus. After extensive washes, the immunoprecipitate was subjected to IEF−SDS−PAGE, and coimmunoprecipitated ARNT was visualized with either mAb 2B10 or rabbit polyclonal antibody on the protein blot. Immunoprecipitation of nuclear extracts after βNF treatment with a control mouse IgG revealed no detectable ARNT on a protein blot, indicating that ARNT's presence in the coimmunoprecipitates is due to immune-specific absorption.[2] There was a significant shift of p*I* toward the basic end for ARNT isoforms heterodimerized with the AhR, compared with ARNT from cytosolic extracts (Figure 3). When ARNT was visualized with 2B10 as the primary antibody, there were ARNT isoforms ranging from p*I* 6.1 to 6.8, with the predominant isoform at p*I* 6.8 (Figure 3A). This was a significant p*I* shift of 0.6 unit (from p*I* 6.2 to 6.8) compared with the predominant ARNT isoform present in immunoprecipitates of cytosol (Figure 3C). The immunoprecipitated ARNT visualized with rabbit polyclonal anti-ARNT antibody showed a similar pattern (Figure 3B). ARNT immunoprecipitated from a cytosolic fraction after βNF treatment displayed the same pattern of isoforms as that of untreated Hepa 1 cells.[2] This indicates that there was no change of p*I* for the general population of ARNT in Hepa 1 cells after βNF treatment; thus, the shift of p*I* observed in the nuclear extracts was unique for the subpopulation of ARNT that was heterodimerized with the AhR. The shift of p*I* observed is

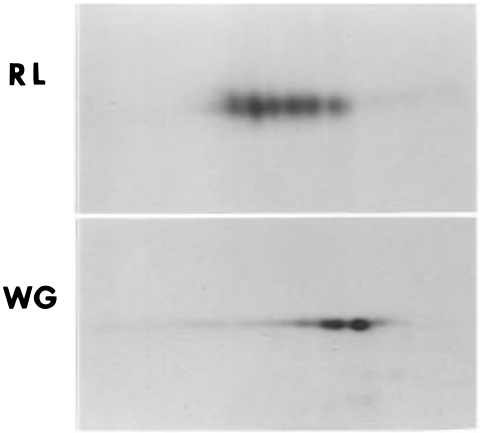

FIGURE 4: *In vitro* expression of ARNT in TNT SP6-coupled rabbit reticulocyte lysate (RL) and wheat germ extract systems (WG). *In vitro* translation of ARNT was performed in the presence of 20 μCi of [^{35}S]methionine per 50 μL reaction mixture. ARNT was visualized by autoradiography.

most likely due to an alteration in posttranslational modifications, such as phosphorylation/dephosphorylation events. During these studies, we were particularly concerned about any phosphatase activity during the isolation of nuclear or cytosolic extracts. A group of phosphatase inhibitors at relatively high concentrations has been used during the homogenization of cells and during immunoprecipitations as described by Papavassiliou (1994). After IEF−SDS−PAGE the level of charge heterogeneity between cytosolic ARNT and ARNT bound to the *Ah* receptor in the nucleus was the same as obtained using buffers with the standard mixture of phosphatase inhibitors.[2]

In Vitro Translated ARNT Exhibits Charge Heterogeneity. ARNT was *in vitro* translated using the pSV-Sport-hARNT plasmid (Dolwick *et al*., 1993) in both rabbit reticulocyte lysate (RL) and wheat germ extract (WG) systems. The reaction was carried out with a SP6 TNT-coupled transcription/translation system, in the presence of [^{35}S]methionine as recommended by the manufacturer. ARNT was translated 3−4 fold more efficiently in the rabbit reticulocyte lysate than in the wheat germ extract system, as is evident in Figure 4. There were significantly more isoforms of ARNT detected in the reticulocyte lysate system; most of them were more acidic, compared to the ARNT from the wheat germ extract system (Figure 4). The ARNT isoforms in reticulocyte lysate span a large p*I* range, from the most acidic forms at p*I* 5.9−6.5 (Figure 4A, top panel). There was no predominant form observed, and the p*I* range detected was smaller than cytosolic ARNT. ARNT isoform heterogeneity was considerably less in the wheat germ extract with only a few relatively basic isoforms observed (Figure 4B, bottom panel). Only two predominant forms were detected, with p*I* 6.4 and 6.6. In addition, there was a shift of p*I* toward the basic end of these isoforms compared to ARNT in Hepa 1 cytosol. ARNT was also visualized with anti-ARNT antibodies and showed the same pattern as autoradiographs.[2]

The rabbit reticulocyte lysate and wheat germ extract are of diverse origins. Therefore, protein synthesis machinery in these two systems is different, including the type and level of posttranslational modifications. The results indicated that ARNT *in vitro* translated in reticulocyte lysate was heavily modified when compared to wheat germ extract. These differences in the p*I* values observed may suggest that certain

posttranslational modifications are functionally important considering that ARNT in wheat germ extract does not form functional heterodimers with AhR translated in rabbit reticulocyte lysate.[2]

In Vitro Formation of AhR/ARNT Heterodimer. In order to test whether a specific ARNT isoform is required for efficient AhR/ARNT dimerization, AhR was *in vitro* transformed[3] by TCDD to heterodimerize with ARNT; this AhR/ARNT heterodimer was capable of binding to DNA in gel shift assays.[2] In the presence of TCDD and DTT, the reaction mixture containing Hepa 1 cytosol was incubated at 30 °C for 2 h. DTT is required for optimal TCDD-mediated AhR/ARNT heterodimerization in *in vitro* transformation assays.[2] This result is consistent with a previous report demonstrating the importance of the redox state of the AhR (Ireland *et al*., 1995). AhR/ARNT heterodimer was coimmunoprecipitated from Hepa 1 cytosol with an anti-AhR rabbit polyclonal antibody (Pollenz *et al*., 1994) after TCDD activation. ARNT was visualized with 2B10, followed by GAM−biotin, and streptavidin−peroxidase complex incubations (Figure 5A). *In vitro* transformation in the presence of DMSO results in a low level of heterodimer formation. Lanes 1 and 2 in Figure 5A represent coimmunoprecipitations of ARNT without TCDD activation with control rabbit IgG or anti-AhR antibody, respectively. After TCDD activation, immunoprecipitations were done with a control rabbit IgG, anti-AhR antibody, or anti-AhR antibody in the presence of phosphatase inhibitors during incubations (Figure 5A, lanes 3−5). These data would indicate that after *in vitro* TCDD activation, a significant level of TCDD/AhR/ARNT heterodimer is formed, and ARNT is efficiently coimmunoprecipitated. The ARNT bands present in lanes 1 and 3 appear to be due to nonspecific ARNT binding to the resin. When a spectrum of phosphatase inhibitors was included in the reaction mix during TCDD activation and in immunoprecipitations, there was no apparent effect on AhR/ARNT heterodimer formation (Figure 5A, lane 5). These results imply that an alteration in the phosphorylation status of AhR and/or ARNT might not be a rate-limiting factor in the dimerization process, at least *in vitro.* AhR that was *in vitro* transformed with TCDD which leads to formation of AhR/ARNT heterodimer was immunoprecipitated with an anti-AhR antibody. The presence of coimmunoprecipitated ARNT was assessed in each sample and compared to the entire cytosolic ARNT pool. The immunoprecipitate was subjected to IEF−SDS−PAGE (Figure 5C). TCDD treatment of Hepa 1 cytosol did not result in a shift in ARNT isoforms immunoprecipitated with mAb 2B10 (Figure 5B) when compared to untreated cytosol.[2] ARNT that heterodimerized with AhR *in vitro* exhibited the same charge heterogeneity pattern as ARNT in the total cytosol pool (Figure 5C). Thus, each isoform is able to heterodimerize with the AhR *in vitro*. Perhaps the shift of ARNT p*I* observed *in vivo* in Hepa 1 nuclear extracts may occur after heterodimerization, and thus be important in other aspects of ARNT regulation (e.g., transactivation).

ARNT Is a Phosphoprotein. Initial attempts to radiolabel ARNT in Hepa 1 cells using [^{32}P]orthophosphate were unsuccessful; we were unable to incorporate a significant amount of radioactivity into the ARNT pool even with overnight cell culture labeling. In addition, [^{32}P]orthophosphate-labeling experiments with transiently transfected mARNT/flag in Hepa 1 cells also resulted in very little radiolabeling of ARNT/flag. The reason for our inability to significantly radiolabel ARNT in Hepa 1 cells is unknown. We decided to utilize a more efficient transfection system, COS-1 cells were transiently transfected with mARNT/flag/pcDNA3 construct. Cells were incubated for 20 h with [^{32}P]-orthophosphate, after the initial 15 h transfection period. ARNT/flag was immunoprecipitated with anti-flag M2 affinity gel; after strigent washes, one immune-specific radiolabeled band was detected by SDS−PAGE (Figure 6A). The results in panels A and B (Figure 6) indicate that we can specifically radiolabel ARNT with [^{32}P]orthophosphate in COS-1 cells transfected with mARNT/flag construct. These immunoprecipitations were also subjected to IEF−SDS−PAGE analysis, and the presence of ARNT on a protein blot was visualized with mAb 2B10 (Figure 6D).

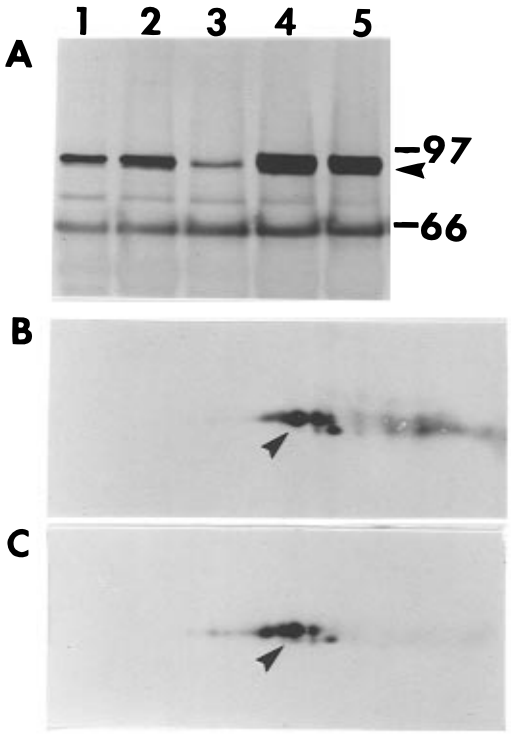

FIGURE 5: *In vitro* transformation of AhR/ARNT heterodimer by TCDD. AhR was *in vitro* activated and heterodimerized with ARNT upon treatment with 20 nM TCDD in Hepa 1 cytosol. ARNT was subsequently coimmunoprecipitated with anti-AhR Ab and subjected to SDS−PAGE (panel A) and IEF−SDS−PAGE analysis (panels B and C). Panel A: Immunoprecipitations from Hepa 1 cytosol were performed with a control rabbit IgG (lanes 1 and 3) and with a rabbit polyclonal anti-AhR Ab (lanes 2, 4, and 5), after treatment with DMSO (lanes 1 and 2) or 20 nM TCDD (lanes 3, 4 and 5) for 2 h at 30 °C. In lanes 1−4, MENG buffer was used during both TCDD treatment and immunoprecipitation, while in lane 5 a spectrum of phosphatase inhibitors was included in the buffers during TCDD treatment and subsequent immunoprecipitation. Panel B: ARNT was coimmunoprecipitated with mAb 2B10 after TCDD treatment of Hepa 1 cytosol. The immunoprecipitate was subjected to IEF−SDS−PAGE, and ARNT was visualized. Panel C: ARNT was coimmunoprecipitated with a rabbit polyclonal anti-AhR Ab after TCDD treatment of Hepa1 cytosol. The immunoprecipitate was subjected to IEF−SDS−PAGE, and ARNT was visualized. ARNT was visualized in the three panels with 2B10, GAM−biotin, and the streptavidin−peroxidase system. The predominant isoform of ARNT observed in Figures 1 and 2 was marked by an arrowhead.

[3] In this report, transformation or transform refers to the process by which the AhR is altered from a non-DNA binding form (9 S) to a DNA binding form (6 S).

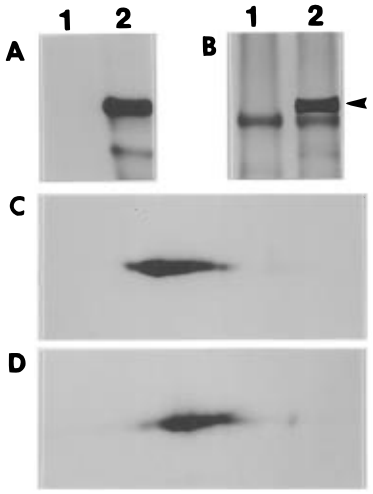

FIGURE 6: Phosphorylation of ARNT in COS-1 cells transiently transfected with mARNT/flag construct. COS-1 cells were transfected with mARNT/flag/pcDNA3 and metabolically labeled with [^{32}P]orthophosphate for 20 h. The cell lysate was subjected to immunoprecipitation with anti-flag M2 mAb affinity gel, and subjected to SDS−PAGE (panels A and B) and IEF−SDS−PAGE analysis (panels C and D). Panels A and C are autoradiographs of the labeled proteins. ARNT/flag was visualized with 2B10 mAb and the GAM−peroxidase conjugate system in panels B and D. In lane 1 of panels A and B, the immunoprecipitations were preincubated with the flag peptide before the cell lysate was added. The ARNT/flag is marked by an arrowhead in panels A and B.

Radiolabeled ARNT was detected by autoradiography (Figure 6C). The results reveal that each isoform of ARNT is labeled in cells with [^{32}P]orthophosphate, with the most predominant signal being detected in the more acidic isoforms. This result is consistent with the concept that the charge heterogeneity detected by IEF−SDS−PAGE is, at least in part, due to phosphorylation. In addition, these results establish the usefulness of COS-1 cells as a system to examine the phosphorylation status of ARNT.

Significance of ARNT Charge Heterogeneity. Previous studies in our laboratory had examined the level of AhR charge heterogeneity (Perdew & Hollenback, 1990; Perdew, 1991). The cytosolic unactivated AhR exists in three isoforms, which appears to be conserved in different cell lines and species. Comparison of the unactivated and the activated heterodimerized AhR indicated that a significant shift in the p*I* of the AhR toward the basic end of the IEF gel occurred. Thus, like ARNT, the AhR also undergoes a shift in p*I* apparently just prior to or after heterodimerization in the nucleus. This may suggest that a common processing event occurs in the nucleus to both components of the transcriptionally active AhR complex. Although highly speculative, these events may be important in the overall transcriptional activation process.

Clearly, further studies will be necessary to elucidate the functional significance of the alteration in p*I* in ARNT after heterodimerization with the AhR in the nucleus. The IEF−SDS−PAGE analysis detailed in this report should complement phosphorylation studies due to the fact that this technique examines the overall level of charge heterogeneity present. Mapping of ARNT phosphorylation sites coupled with site-directed mutagenesis studies should shed light on the functional significance of the results obtained here.

ACKNOWLEDGMENT

We thank Dr. Richard Pollenz for the rabbit anti-AhR and anti-ARNT polyclonal antibodies. We also thank Dr. Oliver Hankinson and Dr. Chris Bradfield for cDNA constructs.

REFERENCES

Antonsson, C., Arulampalam, V., Whitelaw, M. L., Pettersson, S., & Poellinger, L. (1995) *J. Biol. Chem. 270*, 13968−13972.
Burbach, K. M., Poland, A., & Bradfield, C. A. (1992) *Proc. Natl. Acad. Sci. U.S.A. 89*, 8185−8189.
Chen, H.-S., & Perdew, G. H. (1994) *J. Biol. Chem. 269*, 27554−27558.
Dolwick, K. M., Swanson, H. I., & Bradfield, C. A. (1993) *Proc. Natl. Acad. Sci. U.S.A. 90*, 8566−8570.
Fujii-Kuriyama, Y., Imataka, H., Sogawa, K., Yasumoto, K.-I., & Kikuchi, Y. (1992) *FASEB J. 6*, 706−710.
Fukunaga, B. N., Probst, M. R., Reisz-Porszasz, S., & Hankinson, O. (1995) *J. Biol. Chem. 270*, 29270−29278.
Hapgood, J., Cuthill, S., Denis, M., Poellinger, L., & Gustafsson, J.-A. (1989) *Proc. Natl. Acad. Sci. U.S.A. 86*, 60−64.
Hord, N. G., & Perdew, G. H. (1994) *Mol. Pharmacol. 46*, 618−626.
Huang, Z. J., Edery, I., & Rosbash, M. (1993) *Nature 364*, 259−262.
Ireland, R. C., Li, S.-Y., & Dougherty, J. J. (1995) *Arch. Biochem. Biophys. 319*, 470−480.
Jain, S., Dolwick, K. M., Schmidt, J. V., & Bradfield, C. A. (1994) *J. Biol. Chem. 269*, 31518−31524.
Li, H., Ko, H. P., & Whitlock, J. P., Jr. (1996) *J. Biol. Chem. 271*, 21262−21267.
Lindebro, M. C., Poellinger, L., & Whitelaw, M. L. (1995) *EMBO J. 14*, 3528−3539.
Matsushita, N., Sogawa, K., Ema, M., Yoshida, A., & Fujii-Kuriyama, Y. (1993) *J. Biol. Chem. 268*, 21002−21006.
O'Farrell, P. H. (1975) *J. Biol. Chem. 250*, 4007−4021.
Papavassiliou, A. G. (1994) *J. Immunol. Methods 170*, 67−73.
Perdew, G. H. (1988) *J. Biol. Chem. 263*, 13802−13805.
Perdew, G. H., & Hollenback, C. E. (1990) *Biochemistry 29*, 6210−6214.
Perdew, G. H. (1991) *Arch. Biochem. Biophys. 291*, 284−290.
Pollenz, R. S., Sattler, C. A., & Poland, A. (1994) *Mol. Pharmacol. 45*, 428−438.
Reisz-Porszasz, S., Probst, M. R., Fukunaga, B. N., & Hankinson, O. (1994) *Mol. Cell. Biol. 14*, 6075−6086.
Reyes, H., Reisz-Porszasz, S., & Hankinson, O. (1992) *Science 256*, 1193−1195.
Sogawa, K., Iwabuchi, K., Abe, H., & Fujii-Kuriyama, Y. (1995a) *J. Cancer Res. Clin. Oncol. 121*, 612−620.
Sogawa, K., Nakano, R., Kobayashi, A., Kikuchi, Y., Ohe, N., Matsushita, N., & Fujii-Kuriyama, Y. (1995b) *Proc. Natl. Acad. Sci. U.S.A. 92*, 1936−1940.
Swanson, H. I., & Bradfield, C. A. (1993) *Pharmacogenetics 3*, 213−230.
Wang, G. L., Jiang, B.-H., Rue, E. A., & Semenza, G. L. (1995) *Proc. Natl. Acad. Sci. U.S.A. 92*, 5510−5514.

BI970891W